PERGAMON

International Journal of Heat and Mass Transfer 45 (2002) 157–164

International Journal of HEAT and MASS TRANSFER

www.elsevier.com/locate/ijhmt

# Instability of the Marangoni convection in a liquid bridge with liquid encapsulation under microgravity condition

Mingwei Li *, Danling Zeng, Tingxia Zhu

*College of Thermal Engineering, Library of Chongqing University, Chongqing University, Chongqing 400044, China*

Received 14 December 2000

**Abstract**

Linear stability theory is used to analyze the stability of the basic state solution of Marangoni convection in a liquid bridge with liquid encapsulation. By processing the linear disturbance equations numerically, stability analysis can be evolved to a complex general eigenvalue problem. Inverse iteration algorithm combined with LZ algorithm is employed to solve the complex generalized eigenvalue problem. The results show that the stability of the system can be enhanced greatly by choosing reasonable matching parameters of the two fluid layers. The preferred mode of instability is axial wave number $\alpha = 2, 3$ and 4, which means that the system is more sensitive to the disturbance with larger wave lengths. 

## 1. Introduction

Thermocapillary convection gives strong influence on the crystal growth process under microgravity. Space experiments by Eyer et al. [1] have shown that time-dependent thermocapillary convection will lead to solute segregation which is the underlying cause of striation. Associated with the thermocapillary instabilities for the models such as horizontal liquid layer, horizontal rectangular cavity and liquid bridge many interesting results were obtained by experimental, theoretical and numerical method. As float-zone crystal growth under microgravity is a highly promising method, the liquid bridge (half float-zone) is usually chosen as to be a model to study the thermocapillary convection and its stability [2–12]. The thermocapillary convection in the liquid bridge with liquid encapsulation displays totally different from the single layer liquid bridge. By encapsulation the thermocapillary convection can be reduced and striation-free crystal can be grown [13]. The research on multilayer liquid columns was seldom reported in open literature. Li and Saghir [14] considered two coaxial liquid columns held between two horizontal disks, where the melt-encapsulant and encapsulant-air interfaces are present. The two liquid columns are heated by a ring heater at the middle of the columns with microgravity conditions imposed to eliminate buoyancy convection. Numerical results were offered and the reduction of Marangoni convection in the melt was observed, but they did not discuss the stability of the solution. The asymptotic solution was obtained for the flow and thermal fields for liquid bridge with liquid encapsulation by Li and Zeng [15], and an axially heated example shows that effective reduction of the convection in the inner layer can be achieved through decreasing liquid viscosity of the outer layer, choosing a proper ratio of interface tension temperature coefficient to free surface tension temperature coefficient and thinning the encapsulation layer.

The main aim of the present paper is to study the stability of the asymptotic solution obtained in [15] by linear stability analysis. As a powerful tool inverse iteration algorithm is employed to solve the complex generalized eigenvalue problem. A series of neutral curves are drawn out and the variation of critical Marangoni number with some dimensionless parameters are shown, the stability of the system can be enhanced strongly by properly selection of the fluid of encapsulation.

* Corresponding author. Tel.: +86-023-6541-5008.
*E-mail address:* mwliz@163.net (M. Li).

0017-9310/02/$ - see front matter 
PII: S0017-9310(01)00125-9

**Nomenclature**

| | |
|---|---|
| $A$ | aspect ratio, $R_2/L$ |
| $b$ | radius ratio of inner and outer liquid columns: $b = R_1/R_2$ |
| $B$ | matrix |
| $Bi$ | Biot number, $hR_2/\lambda_2$ |
| $H$ | heat transfer coefficient |
| $L$ | length of liquid bridge |
| $Ma$ | Marangoni number, $Ma = \gamma_2\beta R_2^2/\mu_2\nu_2$ |
| $R_1$ | inner layer radius |
| $R_2$ | outer layer radius |
| $t$ | time |
| $T_a$ | gas temperature |
| $T_c$ | temperature at cold planar face |
| $T_h$ | temperature at hot planar face |
| $p$ | dimensionless pressure |
| $Pr$ | Prandtl number $Pr = \nu_2/\kappa_2$ |
| $r$ | dimensionless radial coordinate |
| $u_i$ | dimensionless radial velocity component for $i$th layer |
| $w_i$ | dimensionless axial velocity component for $i$th layer |
| $z$ | dimensionless axial coordinate |

*Greek symbols*

| | |
|---|---|
| $\beta$ | temperature gradient along $z$ coordinate for interface 2 |
| $\gamma$ | surface tension temperature coefficient |
| $\kappa$ | thermal diffusivity |
| $\lambda$ | thermal conductivity |
| $\mu$ | dynamic viscosity |
| $\nu$ | kinematic viscosity |
| $\rho$ | density |
| $\sigma$ | surface tension and complex eigenvalue |

*Superscript and subscript*

| | |
|---|---|
| * | physical property ratio of liquid $i = 1$ liquid $i = 2$ |
| $j$ | interfaces ($j = 1, 2$) |

## 2. Physical model

Consider two immiscible axisymmetric coaxial liquid columns contained between two planar faces with a distance $L$ apart, as shown in Fig. 1. Let $R_1$ and $R_2$ to be the radius of the inner and the outer liquid columnar surfaces, respectively. The liquids are assumed incompressible Newtonian fluid with density $\rho_i$, thermal diffusivity $\kappa_i$, thermal conductivity $\lambda_i$, kinematic viscosity $\mu_i$ and dynamic viscosity $\nu_i$ ($i = 1, 2$ for liquid 1 and liquid 2, respectively). The liquid–liquid interface 1 and liquid–gas interface 2 are assumed to be smooth and undeformable. The endwalls at $z = \pm L/2$ are maintained at constant temperature $T_h$ and $T_c$, respectively. Let $\beta$ be a measure of the temperature gradient along the liquid–gas interface 2. The outer liquid 2 is surrounded by a passive gas which has negligible density and viscosity. The law of surface tension versus temperature is assumed to be linear:

$$\sigma_j = \sigma_{0j} - \gamma_j(T_j - T_0) \tag{1}$$

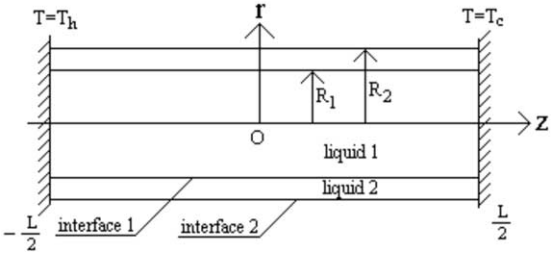


Fig. 1. Physical model.

in which $T_0 = (T_h + T_c)/2$ and $\sigma_{0j}$ is the surface tension of interface $j$ at temperature $T_0$; $\gamma_j$ is the variation rate of surface tension with temperature $T$, where $j = 1$ for the liquid–liquid interface and $j = 2$ for the liquid–gas interface. Gravity is assumed to be absent. We ignore, for the time being, the presence of the endwalls of the zone and concentrate on the study of the convective instability of the core region.

## 3. Formulation and basic state solutions

### 3.1. Formulation

The unsteady axisymmetric motion of liquid $i$ ($i = 1, 2$) is governed by the fundamental equations:

*Continuity equation*:

$$(1/r)(ru_i)_r + w_{iz} = 0. \tag{2a, b}$$

*N–S equation*:

$$u_{it} + u_i u_{ir} + w_i u_{iz} = -(1/\rho_i)p_{ir} + \nu_i(\nabla^2 - 1/r^2)u_i, \tag{2c, d}$$

$$w_{it} + u_i w_{ir} + w_i w_{iz} = -(1/\rho_i)p_{iz} + \nu_i\nabla^2 w_i. \tag{2e, f}$$

*Energy equation*:

$$T_{it} + u_i T_{ir} + w_i T_{iz} = \kappa_i\nabla^2 T_i. \tag{2g, h}$$

Here, $u_i$ and $w_i$ are the velocity components of liquid $i$ in the directions ($r$, $z$), $T_i$ and $p_i$ are the temperature and pressure for liquid $i$, respectively; Laplacian operator, $\nabla$, is defined by

$$\nabla^2 = (1/r)\left(\frac{\partial}{\partial r}\left(r\frac{\partial}{\partial r}\right)\right) + \frac{\partial^2}{\partial z^2}.$$

Eqs. (2a,b)–(2g,h) are subject to the following boundary conditions:

No-slip and isothermal conditions considered at the rigid endwalls,

$$Z = L/2: \quad u_i = w_i = 0, \quad T_i = T_c, \tag{3a–3f}$$

$$Z = -L/2: \quad u_i = w_i = 0, \quad T_i = T_h \tag{3g–3l}$$

on the liquid–liquid interface, $r = R_1$

$$u_1 = u_2 = 0, \tag{3m, 3n}$$
$$w_1 = w_2, \tag{3o}$$
$$T_1 = T_2, \tag{3p}$$
$$\lambda_1 T_{1r} = \lambda_2 T_{2r}, \tag{3q}$$
$$\mu_1 w_{1r} - \mu_2 w_{2r} = -\gamma_1 T_{1z} \tag{3r}$$

on the liquid–gas interface, $r = R_2$

$$u_2 = 0, \tag{3s}$$
$$\mu_2 w_{2r} = -\gamma_2 T_{2z}, \tag{3t}$$
$$-\lambda_2 T_{2r} = h[T_2 - T_a(z)]. \tag{3u}$$

The thermal boundary condition (3u) presumes that the air temperature $T_a(z)$ is known and that the heat transported at the liquid–gas interface can be described by using a heat-transfer coefficient $h$:

The physical quantities are bounded at $r = 0$ as

$$r = 0: \quad u_1, w_1, p_1, T_1 < \infty. \tag{3v–3y}$$

### 3.2. Basic state solutions

By scaling the parameters with proper reference scales ($R_2$ for length, $\gamma_2\beta R_2/\mu_2$ for velocity, $\gamma_2\beta$ for pressure, $\beta R_2$ for temperature $(T_i - T_0)$ and $\mu_2/\gamma_2\beta$ for time), the dimensionless form of system (2a,b)–(2g,h) can be obtained. The approximate analytical solution of steady Marangoni convection in the core region for two coaxial liquid columns under the assumption of linear distribution of the gas temperature $T_a(z) = -z$ was obtained by asymptotical analysis and expressed in dimensionless parameters as:

$$\bar{u}_1 = \bar{u}_2 = 0, \tag{4a, 4b}$$
$$\bar{w}_1 = -C_{11}^{0a}(1 - 2r^2/b^2), \tag{4c}$$
$$\bar{w}_2 = -\left(C_{21}^{0a} + C_{22}^{0a}\ln r + C_{23}^{0a} r^2\right), \tag{4d}$$
$$\bar{p}_1 = (2b^2/C_m)[b^4 - 4b^2\ln b - 1 - (b^5 - 4b^3 + 4b\ln b + 3b)\gamma^*](-z), \tag{4e}$$
$$\bar{p}_2 = [2/\mu^* C_m][2b^2\mu^* - b^2 - 4\mu^*\ln b + 1 - 2\mu^* - (b^3 - b)\gamma^*](-z), \tag{4f}$$
$$\bar{T}_1 = -z + [AMa/4\kappa^*]\left[C_{11}^{0a}(1 - r^2/(2b^2)) + 4\kappa^* C_{12}^{1T}\right], \tag{4g}$$
$$\bar{T}_2 = -z + AMa[C_{21}^{0a} r^2/4 + C_{22}^{0a}(\ln r - 1)r^2/4 + C_{23}^{0a} r^4/16 + C_{21}^{1T}\ln r + C_{22}^{1T}]. \tag{4h}$$

Quantities with upper bar "–" denote the dimensionless basic state solution. $Ma$ is the Marangoni number, i.e., $Ma = \gamma_2 R_2^2/\mu_2\nu_2$; $b$ denotes the radius ratio of liquid 1 to liquid 2, or $b = R_1/R_2$. Superscript "$*$" stands for the physical property ratio of liquid 1 to liquid 2. (e.g., $\mu^* = \mu_1/\mu_2$), and symbol $\gamma^*$ is defined as $\gamma_1/\gamma_2$. $A$ is the aspect ratio $A = R_2/L$. Symbols $C_m$, $C_{11}^{0a}$, $C_{21}^{0a}$, $C_{22}^{0a}$, $C_{23}^{0a}$, $C_{12}^{1T}$, $C_{21}^{1T}$, $C_{22}^{1T}$ are complicated functions of parameters $\mu^*$, $\kappa^*$, $\gamma^*$, $b$ and $Bi$, which can be found in [15].

## 4. Linear stability analysis

To do the linear stability analysis, infinitesimal disturbances $q'(r,z,t)$ are introduced to the system, thus any physical variable, $q(r,z,t)$, is expressed in the form of $q(r,z,t) = \bar{q}(r,z) + q'(r,z,t)$, where $\bar{q}(r,z)$ is the basic state solution. The normal mode will be of the form (dropping primes)

$$q(r,z,t) = \hat{q}(r)\exp(\mathrm{i}\alpha z + \sigma t) \tag{5}$$

in which $\alpha$ is axial disturbance wave number. The complex eigenvalue $\sigma = \sigma_R + \mathrm{i}\sigma_I$ contains the growth rate $\sigma_R$ and the phase speed $\sigma_I = \sigma_I/\alpha$ of the disturbance wave. Thus, the disturbance equations in normal-mode form can be written as:

$$\hat{u}_{ir} + \hat{u}_i/r + i\alpha\hat{w}_i = 0, \tag{6a, 6b}$$
$$ZH_i(\hat{u}_{irr} + \hat{u}_{ir}/r - \alpha^2\hat{u}_i - \hat{u}_{ir}/r^2) - \mathrm{i}\alpha MaP_r^{-1}\bar{w}_i\hat{u}_i - ZG_i\hat{p}_{ir} = MaPr^{-1}\sigma\hat{u}_i, \tag{6c, 6d}$$
$$ZH_i(\hat{w}_{irr} + \hat{w}_{ir}/r - \alpha^2\hat{w}_i) - \mathrm{i}\alpha MaP_r^{-1}\bar{w}_i\hat{w}_i - Map_r^{-1}D\bar{w}_i\hat{u}_i - i\alpha ZG_i\hat{p}_{ir} = MaPr^{-1}\sigma\hat{w}_i, \tag{6e, 6f}$$
$$TH_i(\hat{T}_{irr} + \hat{T}_{ir}/r - \alpha^2\hat{T}_i) - \mathrm{i}\alpha Ma\bar{w}_i\hat{T}_i - Ma\bar{T}_{iz}\hat{w}_i - Ma\bar{T}_{iz}\hat{u}_i = Ma\sigma\hat{T}_i, \tag{6g, 6h}$$
$$r = b: \quad \hat{u}_1 = \hat{u}_2 = \hat{w}_1 - \hat{w}_2 = \hat{T}_1 - \hat{T}_2 = \lambda^* D\hat{T}_1 - D\hat{T}_2 = D\hat{w}_1 - D\hat{w}_2/\mu^* + \mathrm{i}\alpha\gamma^*/\mu^* = 0, \tag{6i–6n}$$
$$r = 1: \quad \hat{u}_2 = D\hat{w}_2 + \mathrm{i}\alpha\hat{T}_2 = D\hat{T}_2 + Bi\hat{T}_2 = 0, \tag{6o–6q}$$
$$r = 0: \quad \hat{u}_1 = D\hat{w}_1 = D\hat{T}_1 = 0, \tag{6r–6t}$$

where $Pr$ is Prandtl number of the outer fluid layer, or $Pr = \nu_2/\kappa_2$, $D = \mathrm{d}/\mathrm{d}r$, $ZG_1 = 1/\rho^*$, $ZG_2 = 1$, $ZH_1 = \nu^*$, $ZH_2 = 1$, $TH_1 = \kappa^*$, $TH_2 = 1$. Eqs. (6a,6b)–(6r–6t) constitute a set of complicated ordinary-differential equations which involve the dependency of $\sigma$ on time $t$.

In order to determine the change of $\sigma$ with varying $Ma$ in parameter space, we construct a discrete version using finite-difference approximation on staggered grids by the primitive variable method, which is a complex, generalized eigenvalue problem of the form:

$$Ax = \sigma Bx, \tag{7}$$

where $x$ is a $(4N-6)$ dimensional column vector of unknown velocity, temperature and pressure at the nodes of the appropriate grid. ($N$ is the number of half section through the axle, $N = N_1 + N_2$, $N_1$ for inner layer and $N_2$ for outer layer, respectively), $A$ and $B$ are $(4N-6) \times (4N-6)$ complex matrices. $A$ is a complicated band matrix. $A$ and $B$ can be partitioned as

$$A = \begin{bmatrix} A_{11} & A_{12} \\ A_{21} & A_{22} \end{bmatrix}, \quad B = \begin{bmatrix} B_{11} & 0 \\ 0 & 0 \end{bmatrix}$$

with $A_{11}$, $B_{11} \in C_{m,m}$ and $A_{22} \in C_{n,n}$. Here $m$ is the number of unknown velocities and temperatures, $m = 3N-6$, $n$ is the number of unknown pressures, $n = N$. $B_{11}$ is a diagonal matrix.

## 5. Numerical procedure

The procedure of stability analysis in this paper is to fix the values of $\mu^*$, $\rho^*$, $\lambda^*$, $\kappa^*$, $\gamma^*$, $Pr$, $Bi$, $b$ as well as the axial wave number $\alpha$ and search for the eigenvalues of system (7) with largest real part of $\sigma^*$ in varying the value of $Ma$. We take $Ma^*$ corresponding to $\sigma_R^* = 0$, represents the value above which the infinitesimal disturbances with axial wave number, $\alpha$, will grow. The critical Marangoni number, $Ma_c$, is the global minimum of $Ma^*$ over $\alpha$ in parameter space defined by

$$Ma_c(\mu^*, \rho^*, \lambda^*, \kappa^*, \gamma^*, Pr, Bi, b) = \min_{\alpha} Ma^*(\mu^*, \rho^*, \lambda^*, \kappa^*, \gamma^*, Pr, Bi, b, \alpha)$$

above which the system will lose its stability. Obviously, the key of our stability analysis is to find out the critical value, $Ma_c$, at which an eigenvalue crosses the imaginary axis first. Since it is expected that this corresponds to a simple Hopf bifurcation point, there should be exactly one complex-conjugate eigenvalue pair with nonzero imaginary part, termed the leading eigenvalue, which crosses the imaginary axis with nonzero speed. The inverse-iteration algorithm is employed in the present computation. The inverse-iteration algorithm is a very efficient method to compute selected eigenvalues and eigenvectors of a generalized eigenvalue problem, by which the interesting eigenvalue can be found and the band structure of matrix is not destroyed. A parameter $s$, estimated by LZ algorithm for relatively coarse discretizations, known as the *shift parameter* is introduced. The eigenvalues of the resulting computations are those which are closest to the value of this parameter chosen for a particular computation.

In order to compute the critical Marangoni number for a fixed wave number, the routines ELZHC, ELZVC from STYR library, the routines IVI containing two modified LINPAK routines CGEFA and CGESL, and the routines CMAE and CMBE utilized for the assignment of matrices $A$ and $B$ are employed. In calculation, the node number $N = 40$ is selected after a detailed comparison with other values of $N$, by which the precision is guaranteed.

## 6. Results and discussion

A series of neutral curves and curves for showing the variation of critical Marangoni number $Ma_c$ and critical phase speed $Cr_c$ with physical parameters are drawn out. Neutral stability curves gives the sufficient condition of loosing stability of the system, this means that the system will be unstable above the neutral curves. For the complex two layer system with multidimensional parameter space, the method used to determine the influence of different dimensionless parameters on the stability of the system is to change one assigned parameter in a certain range with others fixed. For example, if we fixed $\mu^* = 1$, $\rho^* = 1, \ldots,$ this means $\mu_1 = \mu_2$, $\rho_1 = \rho_2$, and so far. Some conclusions can be extracted from Figs. 2–9 as below:

1. As shown in the neutral curves, the stability of the system may change with different parameter matching mode and different wave number. The critical wave numbers $\alpha_c$ corresponding to the minimum of the neutral curves. The system exhibits long wave instability for most cases.
2. The stability of the system could be enhanced by means of (1) increasing the viscosity ratio $\mu^*$, see Fig. 2(b); increasing the density ratio $\rho^*$, see Fig. 3(b); and increasing thermal diffusivity ratio $\kappa^*$, see Fig. 5(b); or (2) decreasing the thermal conductivity ratio $\lambda^*$, see Fig. 4(b).
3. Thinning liquid encapsulation layer will strongly enhanced the stability of the system, see Fig. 9(b). The critical Marangoni number, $Ma$, is 166 at $b = 0.1$, 4563 at $b = 0.6$, 3755 at $b = 0.8$, and then increases sharply when parameter $b$ approaches to 1.
4. The effect of parameter $\gamma^*$ is strong and not monotonous. The most outstanding feature of the plotted $Ma_c - \gamma^*$ curve is tower-like shape as shown in Fig. 6(b), $Ma_c$ is 20 231 at tower top corresponding to $\gamma^* = 0.6$, and varies almost over an order of magnitude. Increasing the difference of the surface tension temperature coefficient $\gamma^*$ will weaken the stability of the system. Choosing properly the value of $\gamma^*$, such as $\gamma^* = 0.3$ to 0.8, may lead to a much more stable system.
5. Biot number $Bi$ and Prandtl number $Pr$ show weak influence on the stability of the system.
6. Among all the parameters, $\gamma^*$ and $b$ may play most important role in the stability of the system. The maximum critical Marangoni number $Ma_c$ obtained by varying $\gamma^*$ and $b$ could be 100 times higher than the minimum value of it.
7. The critical phase speed is defined by $Cr_c = \sigma_{Ic}/\alpha_c$. There exist some relationship between critical phase

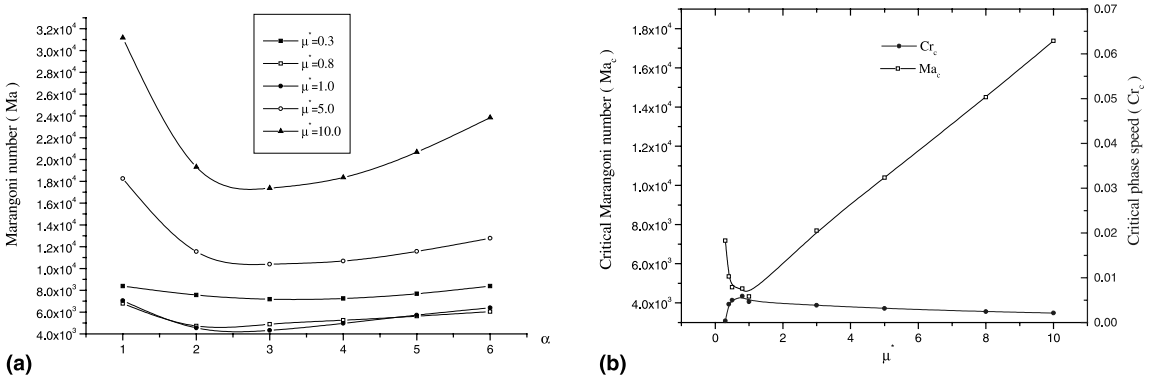


Fig. 2. (a) Neutral curves for various of $\mu^*$ with $\rho^* = \lambda^* = \kappa^* = \gamma^* = Pr = 1$, $Bi = 0$, $b = 0.9$. (b) Critical Marangoni number and critical phase speed versus $\mu^*$ with $\rho^* = \lambda^* = \kappa^* = \gamma^* = Pr = 1$, $Bi = 0$, $b = 0.9$.

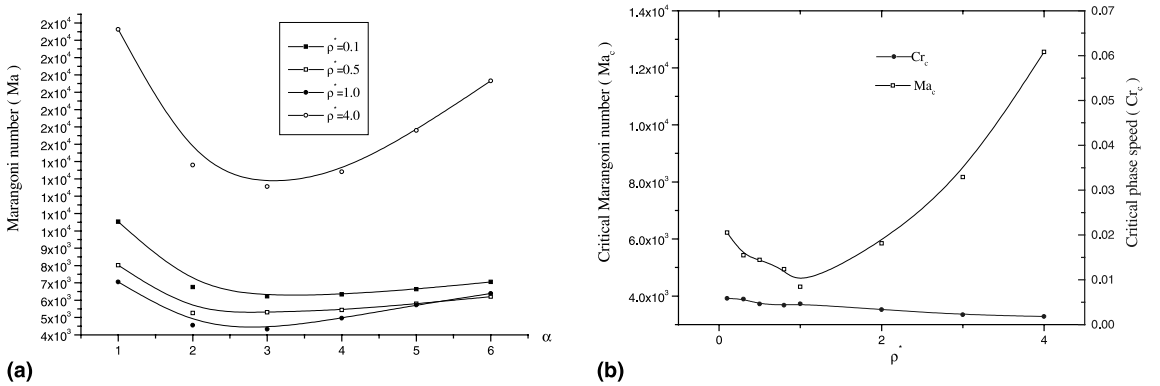


Fig. 3. (a) Neutral curves for various of $\rho^*$ with $\mu^* = \lambda^* = \kappa^* = \gamma^* = Pr = 1$, $Bi = 0$, $b = 0.9$. (b) Critical Marangoni number and critical phase speed versus $\rho^*$ with $\mu^* = \lambda^* = \kappa^* = \gamma^* = Pr = 1$, $Bi = 0$, $b = 0.9$.

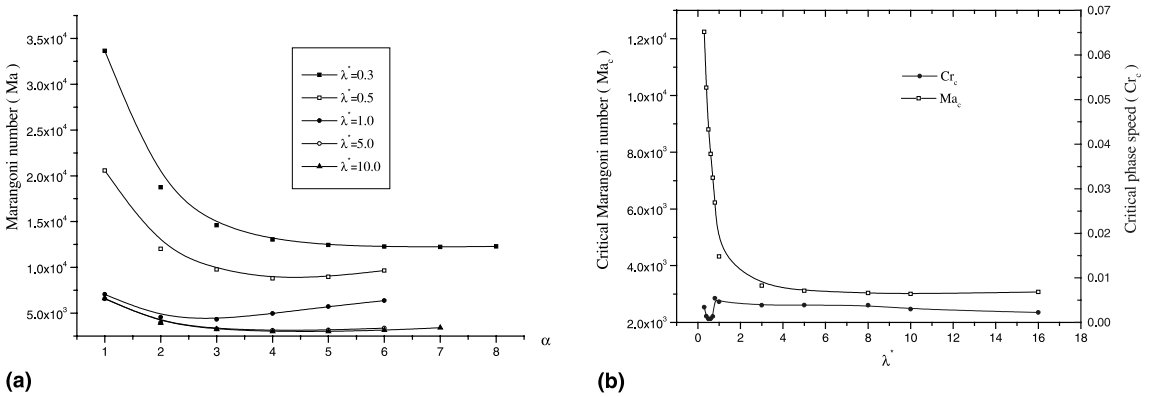


Fig. 4. (a) Neutral curves for various of $\lambda^*$ with $\mu^* = \rho^* = \kappa^* = \gamma^* = Pr = 1$, $Bi = 0$, $b = 0.9$. (b) Critical Marangoni number and critical phase speed versus $\lambda^*$ with $\mu^* = \rho^* = \kappa^* = \gamma^* = Pr = 1$, $Bi = 0$, $b = 0.9$.

speed and critical frequency $f_c = \alpha_c Cr_c/2\pi$. One can see from Figs. 2(b), 3(b), 4(b), 5(b), 6(b), 7(b), 8(b), 9(b)), the change of the critical phase speed with parameters $\mu^*$, $\lambda^*$, $\kappa^*$, $\gamma^*$, $Bi$, and $b$ is not monotonous. In some cases higher critical Marangoni number corresponds to lower critical phase speed as shown in Figs. 2(b), 5(b), 6(b) and 9(b). The dependency of critical phase speed on parameters $\gamma^*$ and

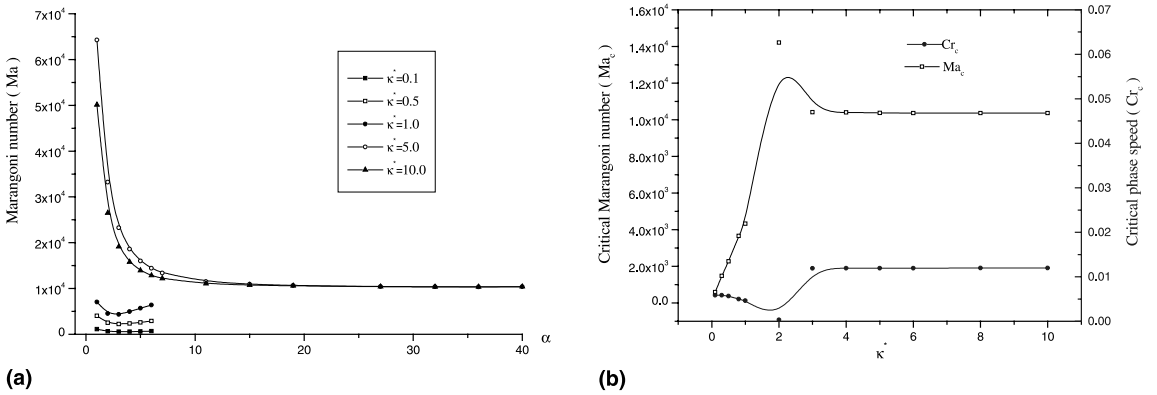


Fig. 5. (a) Neutral curves for various of $\kappa^*$ with $\mu^* = \rho^* = \lambda^* = \gamma^* = Pr = 1$, $Bi = 0$, $b = 0.9$. (b) Critical Marangoni number and critical phase speed versus $\kappa^*$ with $\mu^* = \rho^* = \lambda^* = \gamma^* = Pr = 1$, $Bi = 0$, $b = 0.9$.

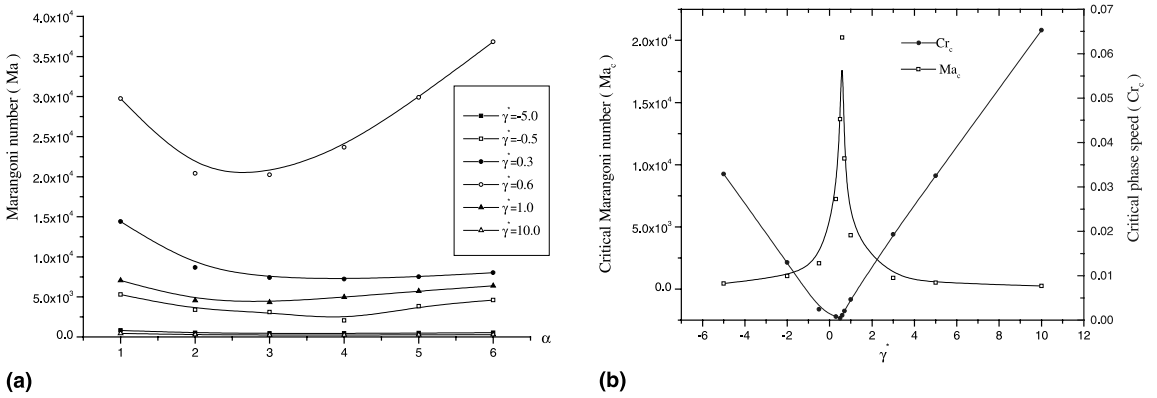


Fig. 6. (a) Neutral curves for various of $\gamma^*$ with $\mu^* = \rho^* = \lambda^* = \kappa^* = Pr = 1$, $Bi = 0$, $b = 0.9$. (b) Critical Marangoni number and critical phase speed versus $\gamma^*$ with $\mu^* = \rho^* = \lambda^* = \kappa^* = Pr = 1$, $Bi = 0$, $b = 0.9$.

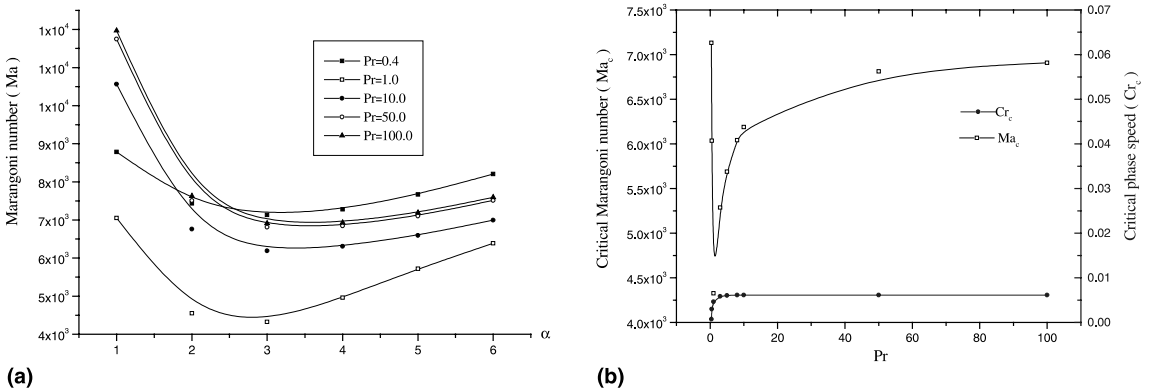


Fig. 7. (a) Neutral curves for various of $Pr$ with $\mu^* = \rho^* = \lambda^* = \kappa^* = \gamma^* = 1$, $Bi = 0$, $b = 0.9$. (b) Critical Marangoni number and critical phase speed versus $Pr$ with $\mu^* = \rho^* = \lambda^* = \kappa^* = \gamma^* = 1$, $Bi = 0$, $b = 0.9$.

$b$ is more remarkable as shown in Figs. 6(b) and 9(b). Biot number $Bi$ and $\rho^*$ show a weak effect on the critical phase speed.

8. Under liquid encapsulation, the system displays totally different behavior from the single-layer case. Because of the extension of the parameter space for the double

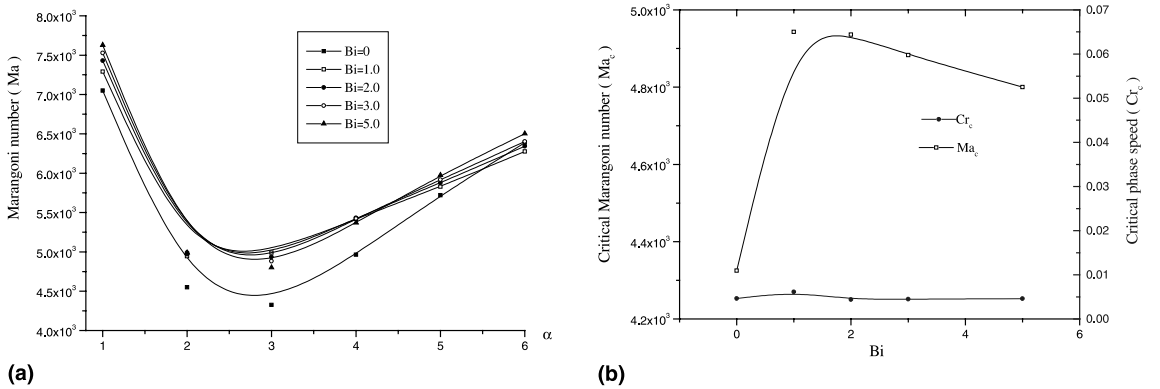


Fig. 8. (a) Neutral curves for various of $Bi$ with $\mu^* = \rho^* = \lambda^* = \kappa^* = \gamma^* = Pr = 1$, $b = 0.9$. (b) Critical Marangoni number and critical phase speed versus $Bi$ with $\mu^* = \rho^* = \lambda^* = \kappa^* = \gamma^* = Pr = 1$, $b = 0.9$.

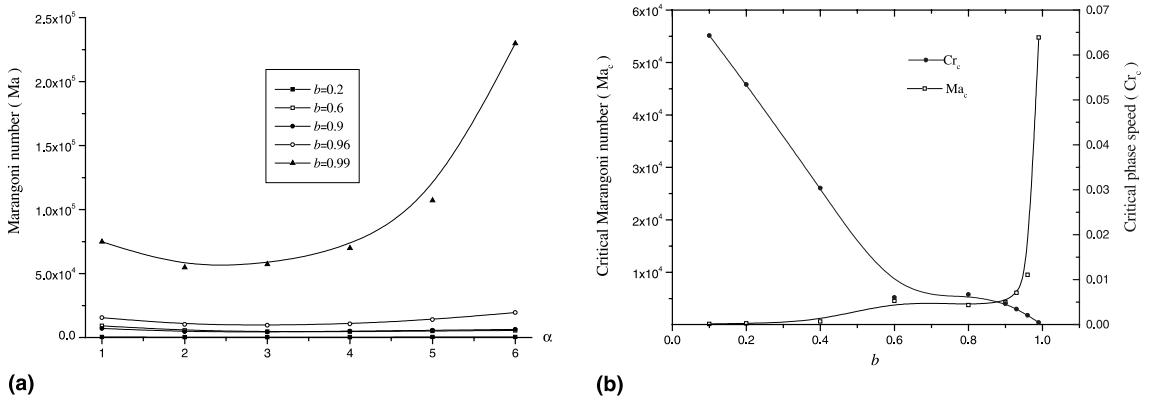


Fig. 9. (a) Neutral curves for various of $b$ with $\mu^* = \rho^* = \lambda^* = \kappa^* = \gamma^* = Pr = 1$, $Bi = 0$. (b) Critical Marangoni number and critical phase speed versus $b$ with $\mu^* = \rho^* = \lambda^* = \kappa^* = \gamma^* = Pr = 1$, $Bi = 0$.

layer system, there exists a great variety of matching the parameters of the two fluids, so that the degrees of freedom for controlling the motion of the inner liquid are greatly increased. A proper choice of the parameters and their matching mode would lead to the expected behavior of the system. Calculations show that, even with a limited combination of the parameters offered by the present paper, the critical Marangoni number could vary over a wide range from $O(10^2)$ to $O(10^4)$. Obviously, this is of great importance in engineering practice and provides a means of flexibly controlling Marangoni convection in a liquid system.

It is worthwhile mentioning that, as the end effect is very important, and hence the assumption of non-deformable interfaces should be relaxed.

## 7. Conclusions

1. A mathematical model describing the unsteady axisymmetric thermocapillary convection in two immiscible axisymmetric coaxial liquid columns is proposed in the present paper.
2. By processing properly the linearized disturbance equations using finite-difference approximation, stability analysis can be evolved to a complex generalized eigenvalue problem.
3. Inverse-iteration algorithm is applied successfully to solve the complex generalized eigenvalue problem.
4. Significant results for engineering applications have been obtained which show that the stability of the system can be enhanced greatly by choosing reasonable matching parameters of the two fluid layers. The matching procedure involves increasing the viscosity ratio and density ratio of the two fluids; choosing properly the fluid of encapsulation, so as to possess a large thermal conductivity, small thermal diffusivity and proper temperature coefficient ratio of interface tension to free surface tension, and thinning the encapsulation layer. The preferred modes of instability mostly corresponds to the disturbances with larger wave lengths.

## Acknowledgements

This work is supported by NSFC with Grant No. 59376261.

## References

[1] A. Eyer, H. Leiste, R. Nitsche, Float zone growth of silicon under microgravity in a sounding rocket, J. Crystal Growth 71 (1985) 173–182.
[2] F. Preisser, D. Schwabe, A. Scharmann, Steady and oscillatory thermocapillary convection in liquid columns with free cylindrical surface, J. Fluid Mech. 126 (1983) 545–567.
[3] J.J. Xu, S.H. Davis, Convective thermocapillary instabilities in liquid bridges, Phys. Fluid 27 (5) (1984) 2880.
[4] J.J. Xu, S.H. Davis, Instability of capillary jets with thermocapillarity, J. Fluid Mech. 161 (1985) 1–25.
[5] Y. Shen, G.P. Neitiel, D.F. Janlowski, H.D. Mittelmann, Energy stability of thermocapillary convection in a model of the float-zone crystal-growth process, J. Fluid Mech. 217 (1990) 639–660.
[6] R. Velten, D. Schwabe, A. Scharmann, The periodic instability of thermocapillary convection in cylidrical liquid bridges, Phys. Fluids A 3 (1991) 267.
[7] C.P. Neitzel, K.T. Chang, D.F. Jankonski, H.D. Mittelmann, Linear stability theory of thermocapillary convection in a model of float-zone crystal growth, AAIA-92-0604 (1992).
[8] J.-C. Chen, S.-S. Sheu, Linear stability analysis of thermocapillary convection in liquid bridges using a mixed finite difference-spectral method, Int. J. Numer. Meth. Heat Fluid Flow 5 (1995) 481–494.
[9] G. Chen, A. Lizee, B. Roux, Bifurcation analysis of the thermocapillary convection in cylindrical liquid bridges, in: Proceedings of the 1996 2nd International Workshop on Modelling in Crystal Growth, Durbay, Belg, October 13–16, 1996.
[10] T.E. Morthland, J.S. Walker, Effects of am axial magnetic field on the unsteady thermocapillary convection in floating-zone semiconductor crystal growth, in: Proceedings of the 1997 ASME Fluids Engineering Division Summer Meeting, FEDSM'97, Part 9 (of 24) June 22–26, 1997.
[11] L. Carotenuto, D. Castagnolo, C. Albanese, R. Monti, Instability of thermocapillary convection in liquid bridges, Phys. Fluids 10 (3) (1998) 555–565.
[12] C.L. Cunff, A. Zebib, Thermocapillary-Coriolis instabilities in liquid bridges, in: Proceedings of the 1998 ASME International Mechanical Engineering Congress and Exposition, vol. 361-3, Anaheim, CA, November 15–20, 1998.
[13] A. Eyer, H. Leiste, Striation-free silicon crystal by float-zoning with surface-coated melt, J. Crystal Growth 71 (1985) 249–252.
[14] J. Li, M.Z. Saghir, Thermocapillary convection in liquid encapsulation float zone, in: International Symposium on Microgravity Science and Application, Beijing, China, 1993.
[15] M.W. Li, D.L. Zeng, The effect of liquid encapsulation on the Marangoni convection in a liquid column under microgravity condition, Int. J. Heat Mass Transfer 39 (17) (1996) 3725–3732.